

Constraining the luminosity function parameters and population size of radio pulsars in globular clusters

Jayanth Chennamangalam^{1*}, D. R. Lorimer^{1,2}, Ilya Mandel³
and Manjari Bagchi¹

¹ *Department of Physics, West Virginia University, PO Box 6315, Morgantown, WV 26506, USA*

² *NRAO, Green Bank Observatory, PO Box 2, Green Bank, WV 24944, USA*

³ *School of Physics and Astronomy, University of Birmingham, Edgbaston, Birmingham B15 2TT, UK*

ABSTRACT

Studies of the Galactic population of radio pulsars have shown that their luminosity distribution appears to be lognormal in form. We investigate some of the consequences that occur when one applies this functional form to populations of pulsars in globular clusters. We use Bayesian methods to explore constraints on the mean and standard deviation of the luminosity function, as well as the total number of pulsars, given an observed sample of pulsars down to some limiting flux density, accounting for measurements of flux densities of individual pulsars as well as diffuse emission from the direction of the cluster. We apply our analysis to Terzan 5, 47 Tucanae and M 28, and demonstrate, under reasonable assumptions, that the number of potentially observable pulsars should be within 95.45% credible intervals of 133^{+101}_{-58} , 66^{+55}_{-31} and 109^{+125}_{-63} , respectively. Beaming considerations would increase the true population size by approximately a factor of two. Future cluster pulsar discoveries would allow this method to be used to compare the luminosity function between different clusters.

Key words: methods: numerical — methods: statistical — globular clusters: general — globular clusters: individual: Terzan 5, 47 Tucanae, M 28 — stars: neutron — pulsars: general

1 INTRODUCTION

Globular clusters are spherical collections of stars located throughout the halos of galaxies. Once thought to be composed entirely of old metal-poor population II stars, they are now also believed to precipitate during interactions or collisions of galaxies, therefore containing younger stars having higher metallicities (see Zepf 2003). The total masses of globular clusters range up to the order of $10^6 M_{\odot}$ (see Meylan & Heggie 1997), and core stellar number densities reach 10^6 pc^{-3} . The high core densities lead to dynamical interactions between stellar systems that are found less commonly in the Galactic plane. For example, globular clusters favour the formation of low-mass X-ray binaries (LMXBs) that are believed to be the progenitors of millisecond pulsars (MSPs; Alpar et al. 1982), and hence, the ratio of MSPs to normal pulsars is much larger in globular clusters than in the Galactic field. In addition, the MSPs in globular clusters tend to have higher eccentricities compared to their field counterparts, due to exchange or fly-by encounters. MSPs, due to their formation history, can be considered long-lived

tracers of LMXBs, and therefore, constraints on the MSP content of globular clusters provide unique insights into binary evolution and the integrated dynamical history of globular clusters, while determining the radio luminosity function of these pulsars helps shed light on the radio emission mechanism in action in these compact objects.

Pulsar searches of globular clusters have yielded impressive returns in recent years (see Camilo & Rasio 2005), with currently 143 pulsars known in 27 clusters¹. Of these, three clusters, Terzan 5, 47 Tucanae and M 28 are known to harbour more than 10 pulsars each, the most populous being Terzan 5 with 34 (Ransom S. M., private communication). In this paper, we describe a Bayesian method that we have developed to compute an estimate of the true number of pulsars in a given cluster, given a set of observations. There have been many attempts to constrain the population size of pulsars in all globular clusters in the Galaxy (see, for example, Kulkarni, Narayan & Romani 1990; Bagchi, Lorimer & Chennamangalam 2011). This work is different in that it treats clusters individually instead

* E-Mail: jchennam@mix.wvu.edu

¹ See Paulo Freire's globular cluster pulsar catalogue at <http://www.naic.edu/~pfreire/GCpsr.html>

of dealing with the total population. Bayesian approaches to constrain the pulsar population of individual globular clusters have been used specifically for the case of young (non-recycled) pulsars by Boyles et al. (2011). This work focuses on the entire radio pulsar content of the cluster – the majority of which is made up of old (recycled) pulsars – and additionally, attempts to constrain luminosity function parameters jointly with population size.

Faucher-Giguère & Kaspi (2006) have shown that the luminosity distribution of Galactic pulsars appears to be lognormal in form. More recently, Bagchi et al. (2011) have verified that the observed luminosities of recycled pulsars in globular clusters are consistent with this result. Assuming, therefore, that there is no significant difference between the nature of Galactic and cluster populations, we investigate some of the consequences that occur when one applies this functional form to populations of pulsars in individual globular clusters.

For a lognormal (base-10) distribution of pulsar luminosities, the luminosity function is given by

$$f(\log L) = \frac{1}{\sigma\sqrt{2\pi}} e^{-\frac{(\log L - \mu)^2}{2\sigma^2}}, \quad (1)$$

where L is the luminosity in mJy kpc², μ is the mean and σ is the standard deviation of the distribution. We are interested in the situation where we observe n pulsars with luminosities above some limiting luminosity L_{\min} . Given this sample of pulsars, we ask what constraints we can place on their luminosity function parameters, in addition to the potentially observable population size N (that is, the population of pulsars beaming towards the Earth). Another way of thinking about this problem is that there is a family of luminosity function parameters and population sizes that is consistent with an observation of n pulsars above the luminosity limit of the survey, and we are analyzing the posterior probabilities of different members of this family given the observations.

This paper is organized as follows: In §2, we describe our technique. In §3, we apply the technique to observations of a few globular clusters to determine the constraints on the luminosity function parameters and population size. Later, we refine our results using *a priori* information on the luminosity function parameters to get a better estimate of the number of pulsars in those clusters. A summary and our conclusions are presented in §4.

2 BAYESIAN PARAMETER ESTIMATION

Bayes' theorem (see Wall & Jenkins 2003; Gregory 2005), for the purpose of parameter estimation, can be stated mathematically as

$$p(\boldsymbol{\theta}|D, M) = \frac{p(D|\boldsymbol{\theta}, M)p(\boldsymbol{\theta}|M)}{p(D|M)}, \quad (2)$$

where $\boldsymbol{\theta}$ is a set of parameters, D is some data and M is a model describing the parameters. In this notation, $p(\boldsymbol{\theta}|D, M)$ represents the probability of obtaining a set of parameter values given the data and the model, and is termed the *joint posterior probability density*. Similarly, $p(D|\boldsymbol{\theta}, M)$ is the probability of having obtained the observed data, given the parameter values and the model, and is termed

the *likelihood*, and $p(\boldsymbol{\theta}|M)$, the *a priori* probability dictated by the model, is termed the *prior probability density*. The denominator, $p(D|M)$ is called the *evidence*, and is just a normalizing factor that can be dropped since we are only interested in relative probabilities, thereby giving

$$p(\boldsymbol{\theta}|D, M) \propto p(D|\boldsymbol{\theta}, M)p(\boldsymbol{\theta}|M). \quad (3)$$

In this paper, we use Bayes' theorem to find the joint posterior probability density functions of the model parameters μ , σ and N given some data. In our case, the data are the individual pulsar flux densities that we call $\{S_i\}$, the observed number of pulsars, n and the total diffuse flux density of the cluster, S_{obs} .

Luminosity is a property intrinsic to pulsars, while flux density is the corresponding observable. The relationship between the two quantities is given by

$$L = \frac{4\pi r^2}{\delta} \sin^2\left(\frac{\rho}{2}\right) \int_{\nu_1}^{\nu_2} S_{\text{mean}}(\nu) d\nu, \quad (4)$$

where r is the distance to the pulsar, δ is the pulse duty cycle, ρ is the radius of the pulsar emission cone, $S_{\text{mean}}(\nu)$ is the mean flux density of the pulsar as a function of observing frequency and ν_1 and ν_2 are the bounds of the frequency range over which the pulsar is observed (see Lorimer & Kramer 2005). Due to the uncertainty associated with the beam geometry, the values of δ and ρ are not generally reliable for luminosity calculations. Therefore, we use a simplified model of the luminosity, the 'pseudoluminosity', that is defined as $L_\nu = S_\nu r^2$ at a given frequency ν (the ν subscript on L and S will be dropped for the rest of the paper). As can be inferred from Equation (4) and the aforementioned pseudoluminosity equation, the luminosity function is inevitably corrupted by uncertainties in distance. To mitigate this, we decided to perform our analysis initially in terms of the measured flux densities, and later, use a model of distance uncertainty to convert our results to the luminosity domain. We take the distance to all pulsars in a globular cluster to be the same. The lognormal in luminosity can then alternatively be written in terms of the flux density. The probability of detecting a pulsar with flux density S in the range $\log S$ to $\log S + d(\log S)$ is then given by a lognormal in S as

$$p(\log S) d(\log S) = \frac{1}{\sigma_S\sqrt{2\pi}} e^{-\frac{(\log S - \mu_S)^2}{2\sigma_S^2}} d(\log S), \quad (5)$$

where S is in mJy, and μ_S and σ_S are the mean and standard deviation of the *flux density distribution*. The probability of observing a pulsar above the limit S_{\min} is then

$$\begin{aligned} p_{\text{obs}} &= \int_{\log S_{\min}}^{\infty} p(\log S) d(\log S) \\ &= \frac{1}{2} \operatorname{erfc}\left(\frac{\log S_{\min} - \mu_S}{\sqrt{2}\sigma_S}\right). \end{aligned} \quad (6)$$

Our analysis involves computing three likelihoods in the flux domain based on three sets of data, computing the total likelihood as the product of these three likelihoods, converting this flux domain likelihood to the luminosity domain, and subsequently, applying priors to obtain the posterior. This procedure is depicted graphically in the block diagram of Figure 1.

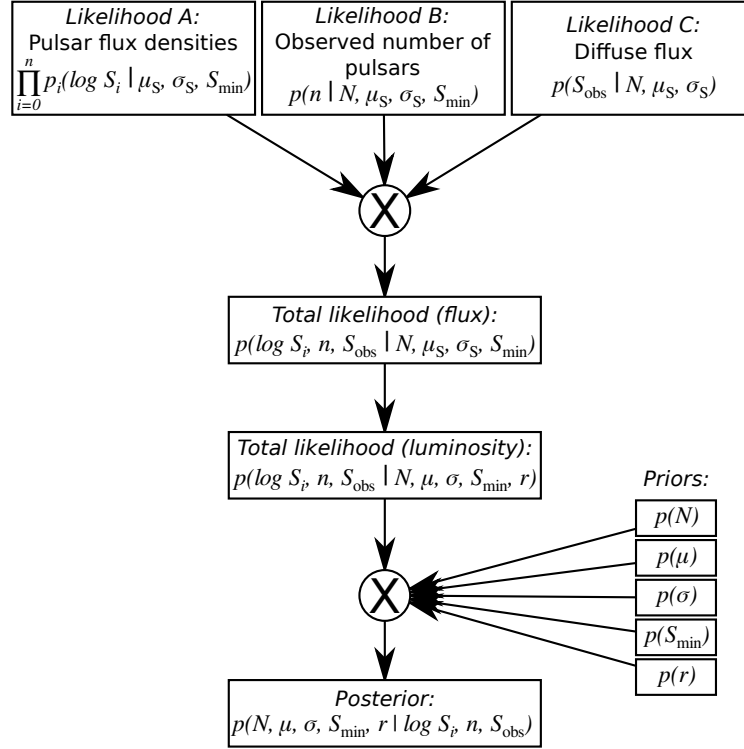


Figure 1. Logical flow of the Bayesian analysis. The circle with the \times sign symbolizes a multiplication operation.

2.1 Using pulsar flux densities

In the first step, we consider as data the measured flux densities of the pulsars in the cluster under scrutiny, that we call $\{S_i\}$. Ideally, the survey sensitivity limit S_{\min} can be taken as another datum, but its exact value is not always known. The effects of radiometer noise, Doppler smearing, interference, and in some cases, interstellar scintillation, result in a distribution of S_{\min} . We decided, therefore, to parametrize S_{\min} . The likelihood of observing a set of pulsars with fluxes $\{S_i\}$ is represented as

$$\prod_{i=1}^n p_i(\log S_i | \mu_S, \sigma_S, S_{\min}),$$

where n is the number of observed pulsars in the cluster. Each term in this product is given by

$$p_i(\log S_i | \mu_S, \sigma_S, S_{\min}) = \frac{1}{p_{\text{obs}} \sigma_S \sqrt{2\pi}} e^{-\frac{(\log S_i - \mu_S)^2}{2\sigma_S^2}} \quad (7)$$

where p_{obs} is as given in Equation (6). This likelihood is represented as ‘Likelihood A’ in Figure 1. Uncertainties in the flux density measurements are not considered here, but it has to be borne in mind that it will have the effect of underestimating the credible intervals on our posteriors.

2.2 Incorporating the number of observed pulsars

To infer the total number of pulsars N in the cluster, we follow Boyles et al. (2011) to take as likelihood the probability of observing n pulsars in a cluster with N pulsars, given by the binomial distribution

$$p(n | N, \mu_S, \sigma_S, S_{\min}) = \frac{N!}{n!(N-n)!} p_{\text{obs}}^n (1 - p_{\text{obs}})^{N-n}, \quad (8)$$

where p_{obs} is computed as in Equation (6). This likelihood is shown as ‘Likelihood B’ in Figure 1.

2.3 Considering diffuse emission

Next, we incorporate information about the observed diffuse flux S_{obs} from the direction of the globular cluster. We assume that all radio emission is due to the pulsars in the cluster, including the both resolved pulsars and the unresolved background. Unlike standard pulsar searches, imaging the diffuse radio emission of a cluster to estimate the number of pulsars therein, is not affected by phenomena that cause pulse broadening, such as dispersion or scattering, or the fact that some of the pulsars in the cluster are in accelerating frames (Fruchter & Goss 1990). For the likelihood of measuring the diffuse flux S_{obs} , we choose

$$p(S_{\text{obs}} | N, \mu_S, \sigma_S) = \frac{1}{\sigma_{\text{diff}} \sqrt{2\pi}} e^{-\frac{(S_{\text{obs}} - S_{\text{diff}})^2}{2\sigma_{\text{diff}}^2}}, \quad (9)$$

where S_{diff} is the expectation of the total diffuse flux of a cluster whose flux density distribution is a lognormal with parameters μ_S and σ_S , and having N pulsars, and σ_{diff} is the standard deviation of this distribution. This likelihood is referred to as ‘Likelihood C’ in Figure 1. Assuming that the cluster contains N pulsars, each having average luminosity,

$$S_{\text{diff}} = N \langle S \rangle, \quad (10)$$

and

$$\sigma_{\text{diff}} = \sqrt{N} \text{SD}(S), \quad (11)$$

where the expectation of S is given by

$$\langle S \rangle = 10^{\mu_S + \frac{1}{2}\sigma_S^2 \ln(10)}, \quad (12)$$

and the standard deviation of S ,

$$\text{SD}(S) = 10^{\mu_S + \frac{1}{2}\sigma_S^2 \ln(10)} \sqrt{10^{\sigma_S^2 \ln(10)} - 1}. \quad (13)$$

We do not consider the uncertainty in the diffuse flux measurement, and as mentioned in §2.1, this has the effect of underestimating the credible intervals on our posteriors.

The total likelihood, then is the product of the three likelihoods computed above, as shown below:

$$\begin{aligned} p(\log S_i, n, S_{\text{obs}} | N, \mu_S, \sigma_S, S_{\text{min}}) \\ = \prod_{i=1}^n p_i(\log S_i | \mu_S, \sigma_S, S_{\text{min}}) \\ \times p(n | N, \mu_S, \sigma_S, S_{\text{min}}) \\ \times p(S_{\text{obs}} | N, \mu_S, \sigma_S). \end{aligned} \quad (14)$$

2.4 Transformation to luminosity domain

The flux density distribution of pulsars in a globular cluster, although proportional to their luminosity distribution, is not suitable for comparing the populations in different clusters, as it depends on the distance to the cluster. It is, therefore, useful to transform the total likelihood obtained in the previous subsection to the luminosity domain. We convert the total likelihood of Equation (14) to the luminosity domain in the following way. Since the pseudoluminosity equation can be written in terms of logarithms as $\log L = \log S + 2 \log r$, where L is in mJy kpc², S is in mJy, and r is in kpc, the means of the two distributions are related additively by the term $2 \log r$, while the standard deviations are the same. Taking into account the uncertainty in distance, we have a distribution of distances, $p(r)$. The total likelihood in the luminosity domain is

$$\begin{aligned} p(\log S_i, n, S_{\text{obs}} | N, \mu, \sigma, S_{\text{min}}, r) \\ = p(\log S_i, n, S_{\text{obs}} | N, \mu_S, \sigma_S, S_{\text{min}}), \end{aligned} \quad (15)$$

where μ and μ_S are related additively as mentioned above, and σ and σ_S are equal. The final joint posterior in luminosity is then given by

$$\begin{aligned} p(N, \mu, \sigma, S_{\text{min}}, r | \log S_i, n, S_{\text{obs}}) \\ \propto p(\log S_i, n, S_{\text{obs}} | N, \mu, \sigma, S_{\text{min}}, r) \\ \times p(N) p(\mu) p(\sigma) p(S_{\text{min}}) p(r). \end{aligned} \quad (16)$$

The prior on N is taken to be uniform from n to ∞ , where the upper limit, for the sake of computation, would be an arbitrarily large value. We also use uniform priors on the model parameters μ and σ . Due to the nature of the uncertainty in determining the exact value of S_{min} , we choose a uniform prior on it in the range $(0, \min(S_i)]$, where the upper limit is the flux density of the least bright pulsar in the cluster. The prior on r is taken to be a Gaussian.

This joint posterior is integrated to obtain the following marginalized posteriors. For brevity, in these equations, D

indicates the complete set of data used in this analysis.

$$p(N | D) = \iiint p(N, \mu, \sigma, S_{\text{min}}, r | D) d\mu d\sigma dS_{\text{min}} dr \quad (17a)$$

$$p(\mu | D) = \iiint p(N, \mu, \sigma, S_{\text{min}}, r | D) dN d\sigma dS_{\text{min}} dr \quad (17b)$$

$$p(\sigma | D) = \iiint p(N, \mu, \sigma, S_{\text{min}}, r | D) dN d\mu dS_{\text{min}} dr \quad (17c)$$

$$p(S_{\text{min}} | D) = \iiint p(N, \mu, \sigma, S_{\text{min}}, r | D) dN d\mu d\sigma dr \quad (17d)$$

$$p(r | D) = \iiint p(N, \mu, \sigma, S_{\text{min}}, r | D) dN d\mu d\sigma dS_{\text{min}} \quad (17e)$$

The joint distribution of the parameters μ and σ is given by marginalizing the joint posterior over N , S_{min} and r , as

$$p(\mu, \sigma | D) = \iiint p(N, \mu, \sigma, S_{\text{min}}, r | D) dN dS_{\text{min}} dr. \quad (18)$$

3 APPLICATIONS

We applied our Bayesian technique² to the globular clusters Terzan 5, 47 Tucanae and M 28 (although the clusters we consider contain only recycled known pulsars, the analysis would remain the same even if there were young pulsars in the sample). The choice of clusters was based on the amount of data available. Terzan 5 is the cluster most-suited for this analysis due to the fact that it has a relatively large number of pulsars for which flux density measurements are available. Although Terzan 5 has 34 known pulsars (Ransom S. M., private communication), we take $n = 25$, the number of pulsars for which we have flux density measurements. The flux densities of the individual pulsars were collected in a literature survey (Bagchi et al. 2011, and references therein), with the values relevant to this work reproduced in Table 1. For Terzan 5, the flux densities we used were scaled from those reported at 1950 MHz by Ransom et al. (2005) and Hessels et al. (2006) to 1400 MHz using a spectral index, $\alpha = -1.9$, using the power law $S(\nu) \propto \nu^\alpha$. Hessels et al. (2007) and Bagchi et al. (2011) discuss the choice of spectral index in detail. The observed diffuse flux density at 1400 MHz is taken to be $S_{\text{obs}} = 5.2$ mJy (the sum of the diffuse flux and the fluxes of point sources as reported by Fruchter & Goss 2000). The priors used were formed in the following ways. The prior on N was chosen to be a uniform distribution in $[n, 500]$, where the upper limit is 150% of the upper limit obtained by Bagchi et al. (2011) (using the values of μ and σ as found by Faucher-Giguère & Kaspi 2006) above their upper limit. We note that this prior is sufficiently wide to ensure that the posterior does not rail against the prior boundaries. We chose uniform distributions in the same range of μ and σ as used by Bagchi et al. (2011)

² The software package that we developed to perform the analysis described in this paper is available freely for download from <http://psrpop.phys.wvu.edu/gcbayes/>.

as our priors. Survey sensitivity limits were not always available, and additionally, due to a variety of factors mentioned in §2.1, for all of our analyses, we took S_{\min} to be a uniform distribution in the range $(0, \min(S_i)]$. The most recent measurement of the distance to Terzan 5, $r = 5.5 \pm 0.9$ kpc (Ortolani et al. 2007), was used to model the distance prior. We modelled the distance prior as a Gaussian with mean 5.5 kpc and standard deviation 0.9 kpc. Figure 2 shows the results of the analysis for Terzan 5. The mode of the marginalized posterior on N , shown in Figure 2(b), is 35 and the median with the surrounding 95.45% credible interval is 92^{+318}_{-64} . As can be seen from Figures 2(b), 2(c) and 2(d), the constraints we obtain on N , μ and σ , respectively, are broad, due to a dearth of flux density measurements. The marginalized posterior on S_{\min} , plotted in Figure 2(e), shows a strong preference for values away from 0 and closer to that of the least bright pulsar observed. The main results are tabulated in Table 2.

For 47 Tucanae and M 28, containing 14 and 9 pulsars each, the individual flux densities used are given in Table 1. We took $S_{\text{obs}} = 2.0$ mJy (1400 MHz flux as reported by McConnell et al. 2004) for 47 Tucanae, and $S_{\text{obs}} = 1.8$ mJy (1400 MHz flux as reported by Kulkarni et al. 1990) for M 28. The priors on N were taken to be uniform in the intervals $[n, 225]$ for 47 Tucanae and $[n, 400]$ for M 28, where the upper limits were computed in the same way as we did for Terzan 5. Priors on S_{\min} were formed as in the case of Terzan 5, in the range $(0, \min(S_i)]$. Distance measurements from the Harris catalogue (Harris 1996, 2010 edition) were used to form the distance priors, with uncertainties taken to be 15%. The main results for these clusters are tabulated in Table 2.

The value of N can be further refined by considering possible dependences on other physical parameters of globular clusters, and such a study will appear in a future paper (Turk et al., in preparation). Note that N is the size of the population of pulsars in the cluster that are beaming towards the Earth. We can include the beaming fraction – the fraction of all pulsars beaming towards us – to refine this estimate. Uncertainties notwithstanding, the beaming fraction of millisecond pulsars is generally thought to be greater than 50% (Kramer et al. 1998). This, together with the fact that most pulsars in globular clusters are millisecond pulsars, imply that the true population size in a cluster is approximately a factor of two more than the potentially observable population size.

3.1 Using prior information

In the framework developed in the previous section, we use broad uniform (non-informative) priors for the mean and standard deviation of the lognormal. This lack of prior information is apparent in Figure 2(b), where N is not very well constrained. Prior information can help better constrain the parameters of interest. Boyles et al. (2011) use models of Galactic pulsars from Ridley & Lorimer (2010) to narrow down μ to between -1.19 and -1.04 , and σ to the range 0.91 to 0.98. We have chosen our priors on μ and σ to be uniform within these ranges. In this case, we have assumed that the luminosity function of globular clusters has the same form as those in the Galactic field. This assumption appears to be justified by reasons elaborated in Bagchi et al. (2011).

Table 1. Flux densities used in the analysis.

Pulsar	1400 MHz Flux Density (mJy)
Terzan 5	
J1748–2446A	1.91 ^a
J1748–2446C	0.68 ^a
J1748–2446D	0.08 ^a
J1748–2446E	0.09 ^a
J1748–2446F	0.07 ^a
J1748–2446G	0.03 ^a
J1748–2446H	0.03 ^a
J1748–2446I	0.05 ^a
J1748–2446J	0.04 ^a
J1748–2446K	0.08 ^a
J1748–2446L	0.08 ^a
J1748–2446M	0.06 ^a
J1748–2446N	0.10 ^a
J1748–2446O	0.23 ^a
J1748–2446P	0.14 ^a
J1748–2446Q	0.05 ^a
J1748–2446R	0.02 ^a
J1748–2446S	0.03 ^a
J1748–2446T	0.04 ^a
J1748–2446U	0.03 ^a
J1748–2446V	0.13 ^a
J1748–2446W	0.04 ^a
J1748–2446X	0.03 ^a
J1748–2446Y	0.03 ^a
J1748–2446ad	0.15 ^b
47 Tucanae	
J0023–7204C	0.36 ^c
J0024–7204D	0.22 ^c
J0024–7205E	0.21 ^c
J0024–7204F	0.15 ^c
J0024–7204G	0.05 ^c
J0024–7204H	0.09 ^c
J0024–7204I	0.09 ^c
J0023–7203J	0.54 ^c
J0024–7204L	0.04 ^c
J0023–7205M	0.07 ^c
J0024–7204N	0.03 ^c
J0024–7204O	0.10 ^c
J0024–7204Q	0.05 ^c
J0024–7203U	0.06 ^c
M 28	
B1821–24A	0.94 ^d
J1824–2452B	0.07 ^d
J1824–2452C	0.17 ^d
J1824–2452D	0.05 ^d
J1824–2452E	0.06 ^d
J1824–2452F	0.08 ^d
J1824–2452G	0.05 ^d
J1824–2452H	0.06 ^d
J1824–2452J	0.07 ^d

^a Based on values reported by Ransom et al. (2005)

^b Based on values reported by Hessels et al. (2006)

^c Camilo et al. (2000)

^d Begin (2006)

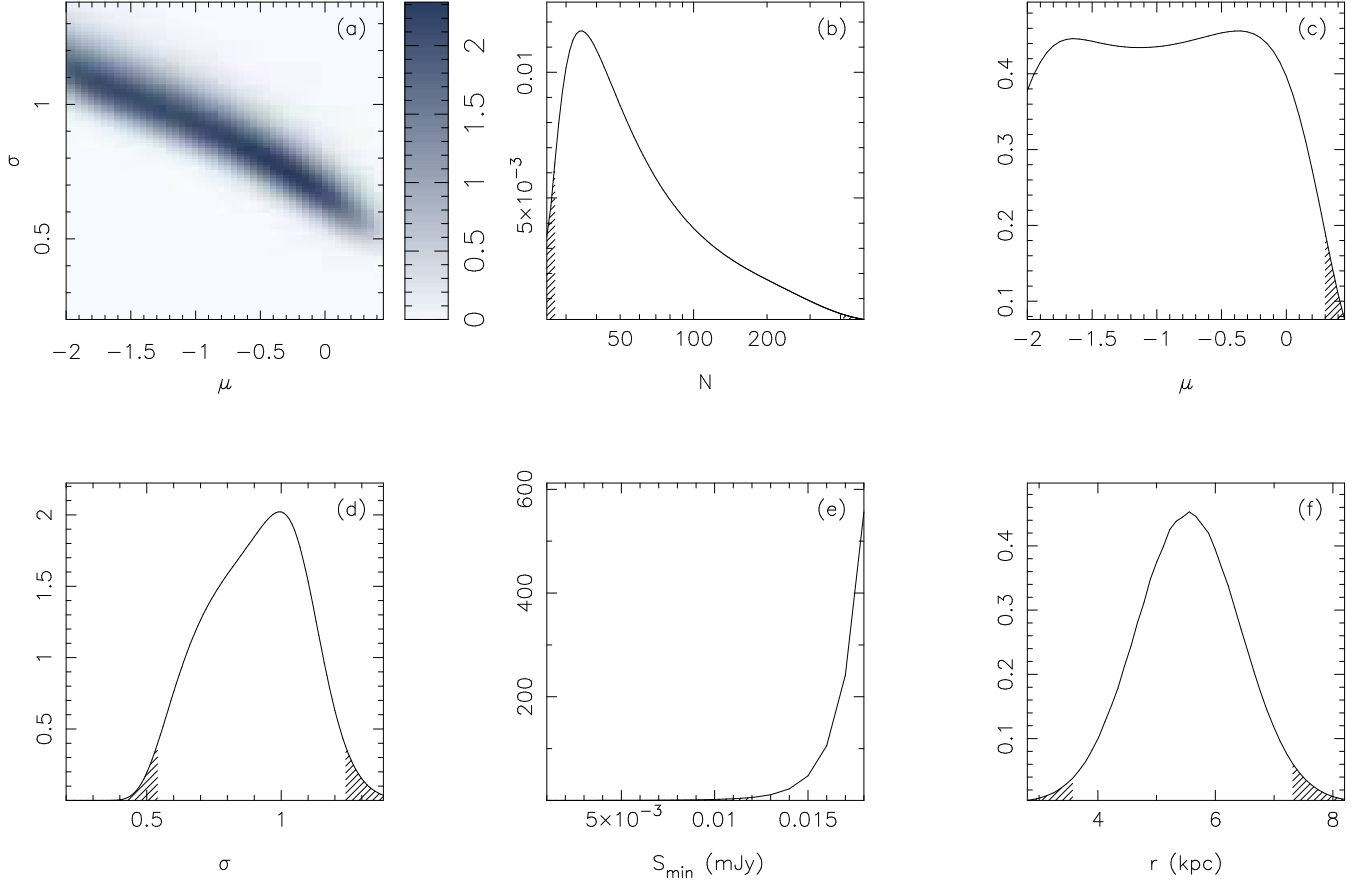


Figure 2. Results of the Bayesian analysis for Terzan 5, with $\{S_i\}$ as given in Table 1, $n = 25$, and $S_{\text{obs}} = 5.2$ mJy. This analysis was run with wide priors on μ and σ , with the ranges equal to those used by Bagchi et al. (2011) (their Figure 2). (a) depicts the joint posterior on μ and σ , marginalized over N , S_{\min} and r as given in Equation (18); (b) is the marginalized posterior for N as given in Equation (17a), with a mode of 35 and a median of 92. The x-axis is plotted in log scale for clarity; (c) is the marginalized posterior for μ as given in Equation (17b) with a mode of -0.35 and a median of -0.9 ; (d) is the marginalized posterior for σ as given in Equation (17c) with a mode of 1.0 and a median of 0.9; (e) is the marginalized posterior for S_{\min} as given in Equation (17d) with both mode and median equal to 0.02 mJy; (f) is the marginalized posterior for r as given in Equation (17e), with a mode of 5.56 kpc and a median of 5.45 kpc. The hatching indicates regions that lie outside a 95.45% credible interval.

Applying the Bayesian analysis over this narrower range of μ and σ for Terzan 5 results in much tighter constraints on N as seen in Figure 3(a), in which the mode of the distribution is 123 and the median and a 95.45% credible interval is 133^{+101}_{-58} . The analysis was also performed for 47 Tucanae and M 28, the results of which are given in Figures 3(b) and 3(c), respectively. For 47 Tucanae, the mode of N is 61 and the median with the surrounding 95.45% credible interval is 66^{+55}_{-31} . For M 28, the mode is 94 and the median with credible interval is 109^{+125}_{-63} . Our result for Terzan 5 is consistent with that of Bagchi et al. (2011). In the case of 47 Tucanae and M 28, there is partial, yet considerable overlap between our credible ranges and the corresponding confidence intervals quoted by Bagchi et al. (2011). For 47 Tucanae, our results agree well with those of Grindlay et al. (2002), i.e., 35–90 MSPs with X-ray luminosities above 10^{30} ergs s^{-1} . The results of our analyses are tabulated in Table 2.

Table 2. Median and credible intervals from the various analyses presented in this paper. We note here that, in addition to the sources of error mentioned in the text, the values of μ and σ presented here are also affected by the fact that computations are discrete and hence use a finite number of steps.

Cluster	N	μ	σ
Wide priors on μ and σ			
Ter 5	92^{+318}_{-64}	$-0.9^{+1.2}_{-1.1}$	$0.9^{+0.3}_{-0.4}$
47 Tuc	25^{+171}_{-11}	$-0.4^{+0.7}_{-1.6}$	$0.6^{+0.5}_{-0.3}$
M 28	195^{+193}_{-167}	$-1.3^{+1.2}_{-0.7}$	$0.8^{+0.3}_{-0.3}$
Narrow priors on μ and σ			
Ter 5	133^{+101}_{-58}	$-1.12^{+0.07}_{-0.07}$	$0.95^{+0.03}_{-0.03}$
47 Tuc	66^{+55}_{-31}	$-1.13^{+0.08}_{-0.06}$	$0.94^{+0.04}_{-0.03}$
M 28	109^{+125}_{-63}	$-1.13^{+0.08}_{-0.06}$	$0.94^{+0.04}_{-0.03}$

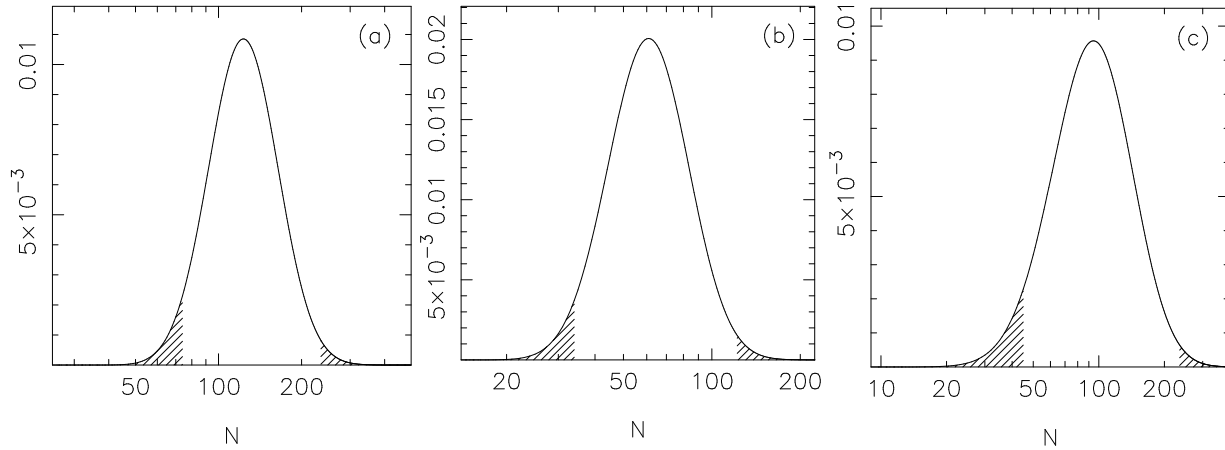


Figure 3. Posteriors on N after applying the Boyles et al. (2011) priors on μ and σ : (a) Terzan 5, with $n = 25$ and $S_{\text{obs}} = 5.2$ mJy. The median with the surrounding 95.45% credible interval of N is 133^{+101}_{-58} ; (b) 47 Tucanae, with $n = 14$ and $S_{\text{obs}} = 2.0$ mJy. The median with credible interval is 66^{+55}_{-31} ; (c) M 28, with $n = 9$ and $S_{\text{obs}} = 1.8$ mJy. The median with credible interval is 109^{+125}_{-63} . The flux densities of the individual pulsars, $\{S_i\}$, used in this analysis are given in Table 1.

4 SUMMARY AND CONCLUSIONS

We have developed a Bayesian technique to constrain the luminosity function parameters and population size of pulsars in individual globular clusters, given a data set that consists of the number of observed pulsars, the flux densities of the individual pulsars in the cluster and the total diffuse flux emission from the direction of the globular cluster, assuming a lognormal luminosity function. We have applied our analysis to a few globular clusters and have demonstrated the utility of this technique in constraining the aforementioned parameters.

Our technique is applied in two different ways – first, with no prior information, and second, assuming prior knowledge of the possible range of μ and σ . As shown for Terzan 5, the results for the first approach do not constrain N , μ or σ very well, but the latter two do exhibit consistency with the values found by Faucher-Giguère & Kaspi (2006) and Bagchi et al. (2011). For the second approach in which we assume prior information to bound μ and σ , the priors help better constrain the total number of pulsars in the cluster.

The technique we have developed here should prove useful in future studies of the globular cluster luminosity function where ongoing and future pulsar surveys are expected to provide a substantial increase in the observed populations of pulsars in many clusters. In particular, we anticipate that the increased amount of data would enable us to constrain the distributions of μ and σ independently (i.e. without the need to assume prior information from the Galactic pulsar population). Further interferometric measurements of the diffuse radio flux in many globular clusters could provide improved constraints on μ and σ by measuring the flux contribution from the individually unresolvable population of pulsars.

ACKNOWLEDGMENTS

We thank Phil Turk and J. C. thanks Nipuni Palliyaguru for useful discussions. This work was supported by a Research Challenge Grant to the WVU Center for Astrophysics by the West Virginia EPSCoR foundation, and also by the Astronomy and Astrophysics Division of the National Science Foundation via a grant AST-0907967.

REFERENCES

- Alpar M. A., Cheng A. F., Ruderman M. A., Shaham J., 1982, *Nat*, 300, 728
- Bagchi M., Lorimer D. R., Chennamangalam J., 2011, *MNRAS*, 418, 477
- Begin S., 2006, Ph.D. Thesis, UBC
- Boyles J., Lorimer D. R., Turk P. J., Mnatsakanov R., Lynch R. S., Ransom S. M., Freire P. C., Belczynski K., 2011, *ApJ*, 742, 51
- Camilo F., Rasio F. A., 2005, in Rasio F. A., Stairs I. H., eds, *ASP Conf. Ser. Vol. 328, Binary Radio Pulsars*. Astron. Soc. Pac., San Francisco, p.147
- Camilo, F., Lorimer D. R., Freire P., Lyne A. G., Manchester R. N., 2000, *ApJ*, 535, 975
- Faucher-Giguère C.-A., Kaspi V. M., 2006, *ApJ*, 643, 332
- Fruchter A. S., Goss W. M., 1990, *ApJ*, 365, L63
- Fruchter A. S., Goss W. M., 2000, *ApJ*, 536, 865
- Gregory P. C., 2005, *Bayesian Logical Data Analysis for the Physical Sciences: A Comparative Approach with Mathematica Support*. Cambridge University Press, Cambridge, UK
- Grindlay J. E., Camilo F., Heinke C. O., Edmonds P. D., Cohn H., Lugger P., 2002, *ApJ*, 581, 470
- Harris W. E., 1996, *AJ*, 112, 1487
- Hessels J. W. T., Ransom S. M., Stairs I. H., Kaspi V. M., Freire P. C. C., 2007, *ApJ*, 670, 363
- Hessels J. W. T., Ransom S. M., Stairs I. H., Freire P. C. C., Kaspi V. M., Camilo F., 2006, *Sci*, 311, 1901

- Kulkarni S. R., Goss W. M., Wolszczan A., Middleditch J., 1990, *ApJ*, 363, L5
- Kulkarni S. R., Narayan R., Romani R. W., 1990, *ApJ*, 356, 174
- Kramer M., Xilouris K. M., Lorimer D. R., Doroshenko O., Jessner A., Wielebinski R., Wolszczan A., Camilo F., 1998, *ApJ*, 501, 270
- Lorimer D. R., Kramer M., 2005, *Handbook of Pulsar Astronomy*, Cambridge Univ. Press, Cambridge, UK
- McConnell D., Deshpande A. A., Connors T., Ables J. G., 2004, *MNRAS*, 348, 1409
- Meylan G., Heggie D. C., 1997, *A&AR*, 8, 1
- Ortolani S., Barbuy B., Bica E., Zoccali M., Renzini A., 2007, *A&A*, 470, 1043
- Ransom S. M., Hessels J. W. T., Stairs I. H., Freire P. C. C., Camilo F., Kaspi V. M., Kaplan D. L., 2005, *Sci*, 307, 892
- Ridley J. P., Lorimer D. R., 2010, *MNRAS*, 404, 1081
- Turk P. J. et al., in preparation
- Wall J. V., Jenkins C. R., 2003, *Practical Statistics for Astronomers*. Cambridge Univ. Press, Cambridge, UK
- Zepf S. E., 2003, in Engvold O., ed, *Highlights of Astronomy*, Vol. 13, as presented at the XXVth General Assembly of the IAU 2003, Astron. Soc. Pac., San Francisco, p. 347